

ESI Support Information

Highly sensitive piezoresistive sensor with interlocked graphene microarrays for meticulous monitoring of human motions

Received 00th January 20xx,
Accepted 00th January 20xx

DOI: 10.1039/x0xx00000x

Lin Cheng, ^{||}^a **Wei Qian,** ^{||}^a **Lei Wei,** ^a **Hengjie Zhang,** ^b **Tingyu Zhao,** ^a **Ming Li,** ^c **Aiping Liu,** ^{*a,d,e} and **Huaping Wu** ^{*b}

^a *Center for Optoelectronics Materials and Devices, Key Laboratory of Optical Field Manipulation of Zhejiang Province, Zhejiang Sci-Tech University, Hangzhou 310018, P. R. China.*

^b *Key Laboratory of Special Purpose Equipment and Advanced Processing Technology, Ministry of Education and Zhejiang Province, College of Mechanical Engineering, Zhejiang University of Technology, Hangzhou 310023, China.*

^c *State Key Laboratory of Structural Analysis for Industrial Equipment, Dalian University of Technology, Dalian 116024, China.*

^d *State Key Laboratory for Strength and Vibration of Mechanical Structures, School of Aerospace Engineering, Xi'an Jiaotong University, Xi'an 710049, P. R. China.*

^e *State Key Laboratory of Digital Manufacturing Equipment and Technology, Huazhong University of Science and Technology, Wuhan 430074, P. R. China.*

*Corresponding author. Tel.: +86 571 86843574; fax: +86 571 86843574.

E-mail address: liuaiping1979@gmail.com, wuhuaping@gmail.com

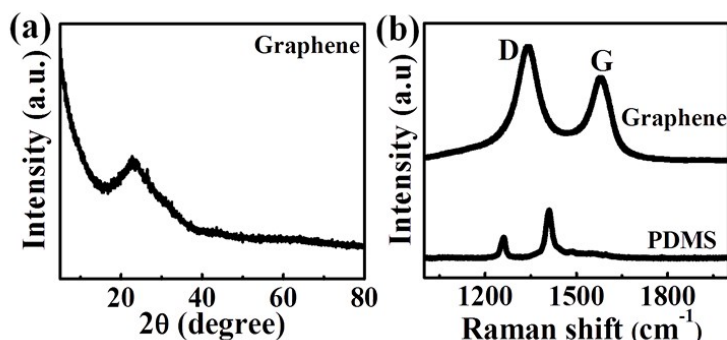


Figure S1. (a) X-ray diffraction (XRD) pattern of drop-coated graphene film. (b) Raman spectra of microstructured PDMS before and after drop-coating of graphene.

The diffraction peak at 23.9° can be assigned to the (002) reflection of graphene (Figure S1a). The characteristic peaks at 1344 cm^{-1} and 1580 cm^{-1} in the Raman spectra (Figure S1b) can be ascribed to D band (represents edges, disordered carbon and defects) and G band (corresponds to vibration of ordered sp^2 -hybridized carbon), suggesting the successful modification of graphene on PDMS.

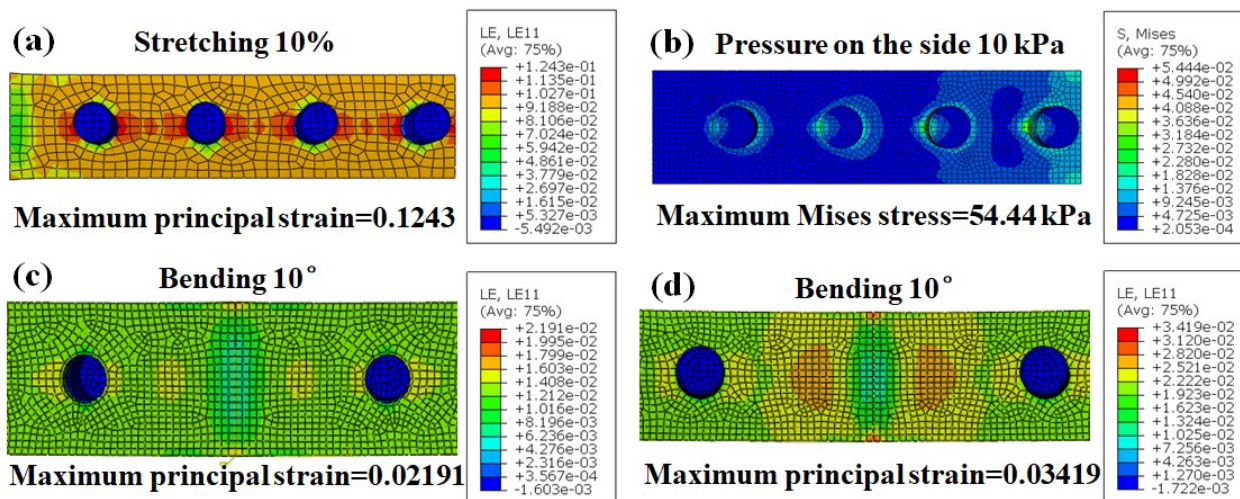


Figure S2. (a) Maximum principal strain, (b) maximum Mises stress, and (c) maximum principal strain of side-contact interlocked sensor under stretching, shear and bending forces. (d) Maximum principal strain of non-interlocked sensor under bending force.

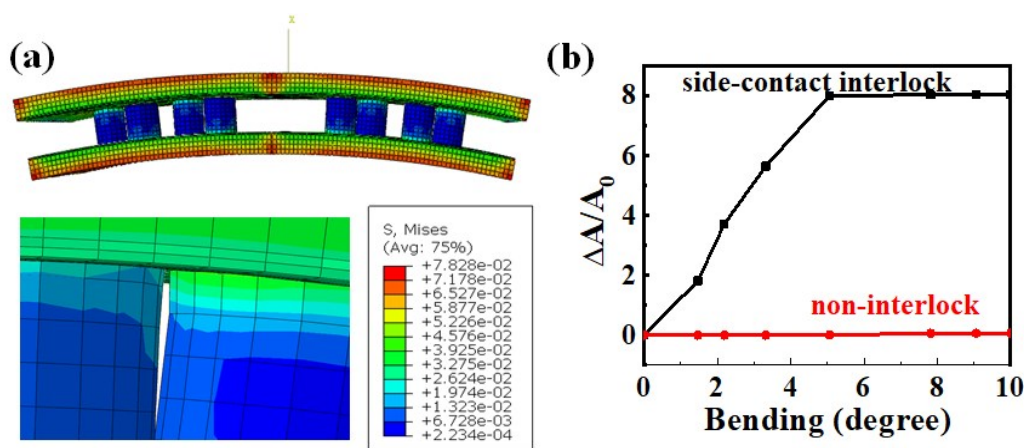


Figure S3. (a) Mises stress distribution of the side-contact interlocked sensor under bending force. (b) The change of area increment with bending angle for the side-contact interlocked and non-interlocked sensors.

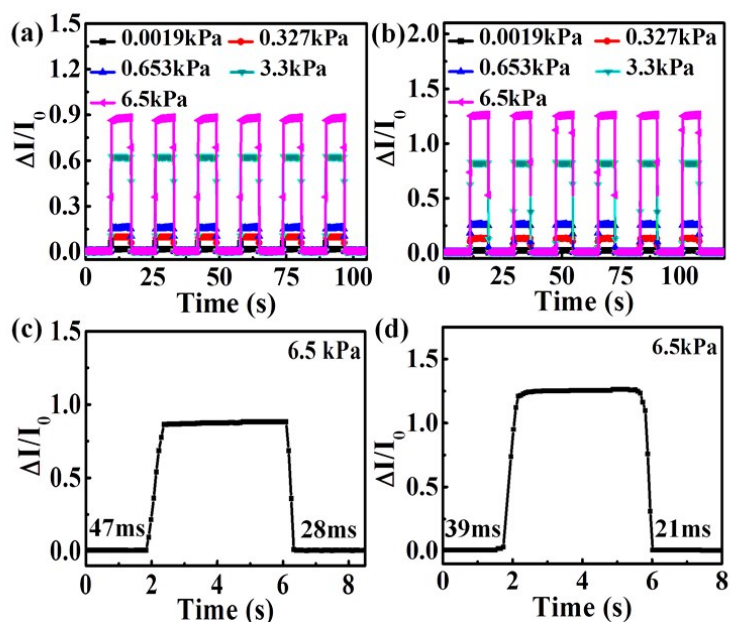


Figure S4. (a)-(b) Relative current changes of (a) planar sensor without microstructures and (b) single microarray sensor under different pressure loadings. (c)-(d) The response time and relaxation time of (c) planar sensor without microstructures and (d) single microarray sensor under a loading of 6.5 kPa.

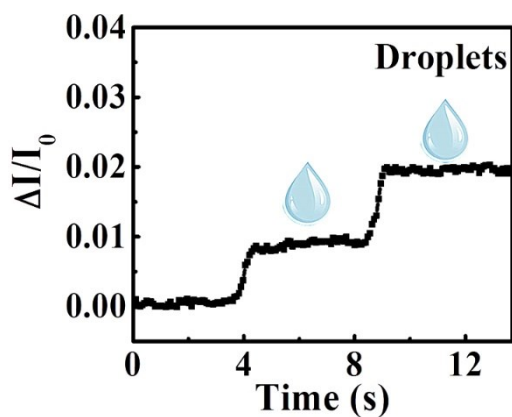


Figure S5. The electrical signal change of side-contact interlocked pressure sensor when a droplet (about 1.0 Pa) was continuously deposited on it.

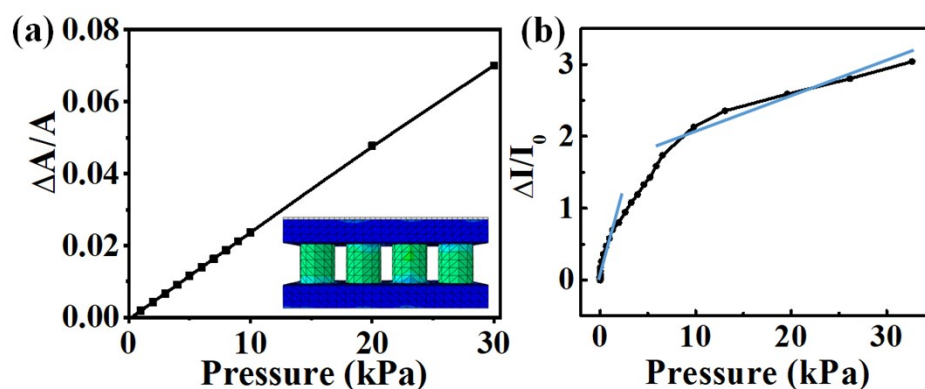


Figure S6. (a) The change of area increment with external pressure and stress distribution and (b) pressure sensitivity for the sensor with non-interlock interposition way.

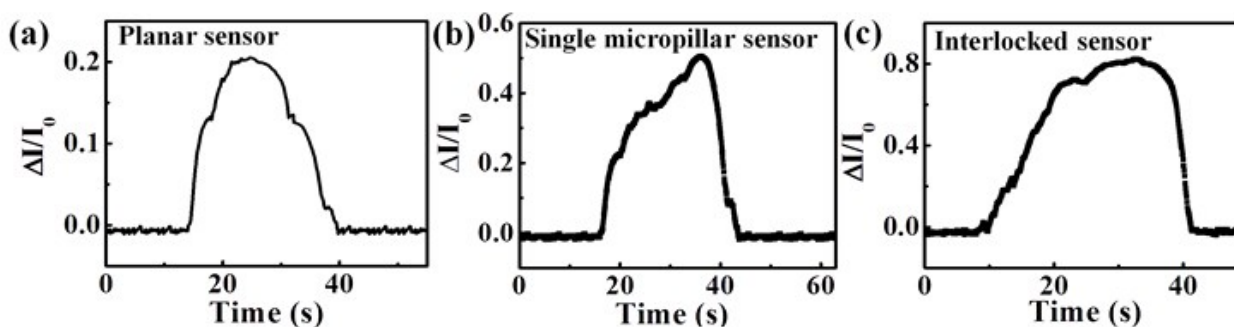


Figure S7. (a,d) Detection of backward bending gesture (low speed) by using different sensors: (a) planar sensor without microstructures, (b) single microarray sensor, and (c) side-contact interlocked sensors.

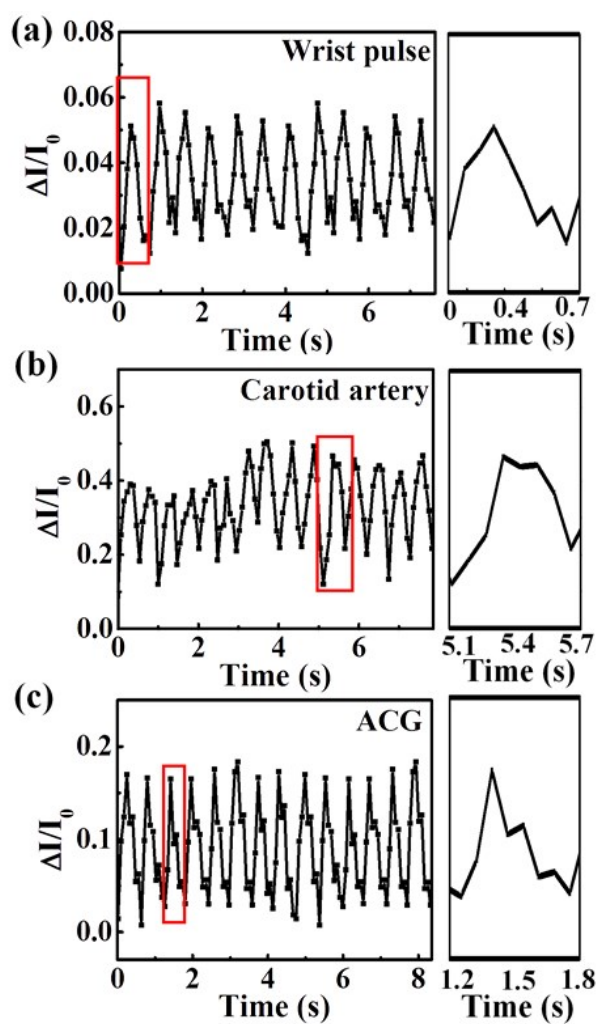


Figure S8. (a) Physiological signal patterns obtained by using side-contact interlocked sensors after exercise condition: (a) wrist pulse, (b) carotid artery, (c) ACG.

Table S1. A brief summary of performances of flexible pressure sensors.

Sensors	Workable range	Sensitivity (kPa ⁻¹)	Response time (ms)	Reference
rGO/PU sponge	9 Pa-10 kPa	0.26 (<2 kPa)	-	(45)
rGO foam	165 Pa-2 kPa	15.2 (<0.3 kPa)	-	(48)
Carbonaceous nanofibrous aerogels	10 Pa-4.5 kPa	0.43 (<3 kPa)	-	(49)
Laser-scribed graphene pressure sensors	-110 kPa	0.96 (<50 kPa)	72	(50)
Double-layered graphene sensors	0.3 Pa-10 kPa	0.24 (<600 Pa)	390	(51)
Conductive fibers coated with dielectric rubber	-10 kPa	0.21 (<2 kPa)	40	(52)
Graphene/PI foam	-6.5 kPa	0.18 (<2 kPa)	-	(53)
Au-Ppy pressure sensors	2 Pa-3 kPa	1.8 (<350 Pa)	-	(54)
Graphene-CNTs hierarchical foam	36 Pa-13 kPa	0.19 (<2.5 kPa)	-	(55)
Interlocked graphene microarray sensors	1.0 Pa-32 kPa	10.41 (<2.5 kPa)	19	Our work

Reference

48. C. Y. Hou, H. Z. Wang, Q. H. Zhang, Y. G. Li and M. F. Zhu, *Adv. Mater.*, 2014, **26**, 5018-5024.
49. Y. Si, S. Q. Wang, C. C. Yan, L. Yang, J. Y. Yu and B. Ding, *Adv. Mater.*, 2016, **28**, 9512-9518.
50. H. Tian, Y. Shu, X. F. Wang, M. A. Mohammad, Z. Bie, Q. Y. Xie, C. Li, W. T. Mi, Y. Yang and T. L. Ren, *Sci. Rep.*, 2015, **5**, 8603-8608.
51. S. Chun, Y. J. Kim, H. S. Oh, G. Bae and W. J. Park, *Nanoscale*, 2015, **7**, 11652-11659.

52. J. Lee, H. Kwon, J. Seo, S. Shin, J. H. Koo, C. Pang, S. Son, J. H. Kim, Y. H. Jang, D. E. Kim and T. Lee, *Adv. Mater.*, 2015, **27**, 2433-2439.
53. Y. Y. Qin, Q. Y. Peng, Y. J. Ding, Z. S. Lin, C. H. Wang, Y. Li, F. Xu, J. J. Li, Y. Yuan, X. D. He and Y. B. Li, *ACS nano*, 2015, **9**, 8933-8941.
54. Q. Shao, Z. Q. Niu, M. Hirtz, L. Jiang, Y. J. Liu, Z. H. Wang and X. D. Chen, *Small*, 2014, **10**, 1466-1472.
55. J. Kuang, Z. H. Dai, L. Q. Liu, Z. Yang, M. Jin and Z. Zhang, *Nanoscale*, 2015, **7**, 9252-9260.